Development of Back-Illuminated, Fully-Depleted CCD Image Sensors For Use in Astronomy and Astrophysics

S.E. Holland, G. Goldhaber, D.E. Groom, W.W. Moses, C.R. Pennypacker, S. Perlmutter, N.W. Wang
Lawrence Berkeley National Laboratory
University of California, Berkeley, CA 94720

R.J. Stover, M. Wei
University of California Observatories/Lick Observatory
University of California, Santa Cruz, CA 95064

Abstract

In this work we investigate the issue of charge spreading in a fully-depleted, back-illuminated CCD fabricated on a high-resistivity silicon substrate. The thickness of the substrate, 300 μm, results in non-negligible charge spreading which is analyzed both theoretically and experimentally.

1. Introduction

We are developing CCD image sensors for astronomy and astrophysics applications [1, 2]. The devices are fabricated on high-resistivity, n-type substrates and are back illuminated. A substrate bias voltage applied to the back-side contact results in full depletion of the 300 μm thick substrate, in contrast to previous deep-depletion CCDs with typically 50 μm thick depletion regions [3–6]. The depletion voltage is relatively low due to the high resistivity of the starting silicon ($\approx$ 10,000 Ω-cm which corresponds to a substrate doping density in the mid-10^{11} cm^{-3} range).

Because of the thickness of the depletion region this device has good quantum efficiency out to a wavelength of 1 μm with negligible fringing [1, 2]. Back illumination is made possible by the development of a simple back-side window consisting of a thin layer of in-situ doped polysilicon with an indium-tin oxide antireflection coating [1, 7]. A phosphorus-doped, back-side polysilicon gettering layer is used to maintain low dark currents, which was a significant problem with initial attempts to develop CCDs on high-resistivity substrates [8, 9].

A concern for the fully-depleted, back-illuminated CCD is spreading via diffusion of the photogenerated charge during the transit from the back side of the device, where short-wavelength light is absorbed, to the CCD potential wells located 300 μm away. In this paper we concentrate on the charge spreading issue, with both theoretical and experimental studies. We derive expressions for charge spreading in the case of an overdepleted substrate as well as in the case where the substrate is only partially depleted. While the latter leads to significant charge spreading and is not a recommended mode of operation, it is shown that useful model parameters can be determined from experimental data in this region.

2. Diffusion in the field region

In this section we analyze the charge spreading for the case of a fully-depleted substrate. Full depletion results in an electric field that extends essentially to the back-side contact. The charge spreading is described by a σ in x and y given by $\sqrt{2Dt_{\rm tr}}$ where D is the diffusion coefficient and $t_{\rm tr}$ is the carrier transit time [10, 11, 12]. Assuming the fields are below the velocity saturation limit, the drift velocity $v_{\rm drift}$ of the charges (holes in this case) is given by

$$v_{\rm drift} = \frac{dy}{dt} = \mu_p E(y) = \mu_p (E_{\rm max} + \frac{\rho_n}{\epsilon_{\rm Si}} y) \qquad (1)$$

where $E(y)$ is the electric field and μ_p is the hole mobility. The expression for $E(y)$ given above is for the case of a simple p^+–n^-–n^+ structure that is overdepleted. $\rho_n = qN_D$ is the volume charge density in the depleted region and $\epsilon_{\rm Si}$ is the permittivity of silicon. N_D is the donor atom density in the depleted region. $E_{\rm max}$ is the field at the p-n junction and is given by

$$E_{\rm max} = -\left(\frac{V_{\rm appl}}{y_D} + \frac{1}{2}\frac{\rho_n}{\epsilon_{\rm Si}} y_D\right) \qquad (2)$$

where $V_{\rm appl}$ is the voltage drop across the drift region and is assumed to be larger than the depletion voltage, $\rho_n {y_D}^2/(2\,\epsilon_{\rm Si})$. The origin is taken at the p-n junction where $E = E_{\rm max}$, and the n^+ region begins at y_D, i.e. y_D is the thickness of the depleted region and $E(y_D) = E_D$.

Solving Eq. 1 and making use of the Einstein relation $D/\mu_p = kT/q$ yields

$$\sigma_{od} = \sqrt{2Dt_{\rm tr}} = \sqrt{2\frac{kT}{q}\frac{\epsilon_{\rm Si}}{\rho_n}\ln\frac{E_{\rm max}}{E_D}} \qquad (3)$$

The subscript indicates that this result is for an overdepleted region. An implicit assumption used in deriving Eq. 3 is that the photons are absorbed at y_D, which is the worst case. A more general derivation would lead to E_D in the above equation being replaced by $E_{\rm max} + (\epsilon_{\rm Si}/\rho_n)y$, where y is the depth at which the photon is absorbed. At high fields σ_{od} approaches the constant-field result

$$\sigma_{od} \approx \sqrt{2\frac{kT}{q}\frac{{y_D}^2}{V_{\rm appl}}} \qquad (4)$$

which is independent of N_D and proportional to y_D. While the above derivation is for a simple p^+–n^-–n^+ structure, the results are also applicable to a fully depleted CCD. The field at the p-n junction of an over-depleted CCD is given by (see Appendix)

$$E_J \equiv -\frac{dV}{dy}(y_J) = -\left(\frac{V_{\rm sub} - V_J}{y_N} + \frac{1}{2}\frac{\rho_n}{\epsilon_{\rm Si}} y_N\right) \quad (5)$$

which is of the same form as Eq. 2. V_J is the potential at the buried channel junction located at y_J, $V_{\rm sub}$ is the substrate bias voltage, and y_N is the thickness of the lightly doped region. For a thick substrate such as used in this work V_J is

$$V_J \approx V_G - V_{FB} - \frac{qN_A}{2\epsilon_{\rm Si}} {y_J}^2 \left(1 + \frac{2\epsilon_{\rm Si} d}{\epsilon_{\rm SiO_2} y_J}\right) \quad (6)$$

where V_G is the gate voltage, V_{FB} is the flatband voltage, N_A is the buried channel doping (assumed to be uniform), and $\epsilon_{\rm SiO_2}$ is the permittivity of the gate insulator of thickness d. This equation predicts that the maximum field in the drift region depends on both applied voltages (V_G and $V_{\rm sub}$) and the channel implant dose $N_A y_J$.

Eq. 5 and 6 are derived from a one-dimensional analysis. For CCDs on high-resistivity silicon the potentials are strongly two dimensional [3, 8] with the effect being that a region exists below the buried channel implant where the field is significantly larger than predicted by Eq. 5. Fig. 1 shows a two-dimensional simulation of one pixel of a high-resistivity CCD. As shown, the potential varies strongly under the collection electrode, where Eq. 5 is no longer valid. As a practical matter the charge spreading in the high-field region is negligible and Eq. 5 can still be used, but V_J is not the potential at the junction but at the point where the field deviates from Eq. 5. The thickness of the drift region will be less than y_N by about 5-10 μm according to Fig. 1.

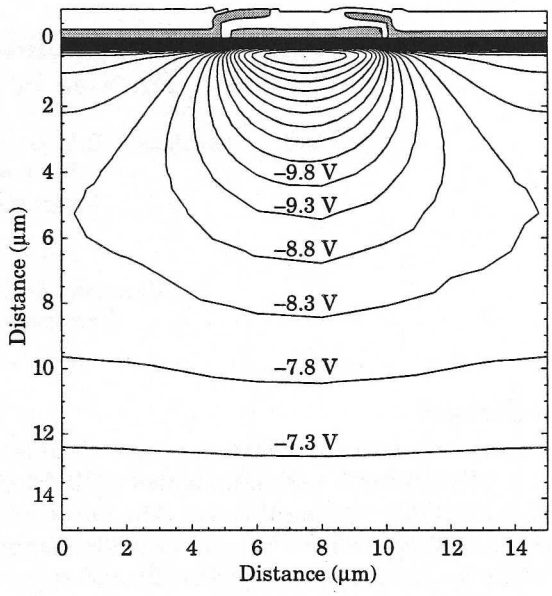

Figure 1: Two-dimensional simulation of one pixel of a CCD on high-resistivity silicon. Equipotential lines are shown at a spacing of 0.5V. The collecting gate is biased at -5V and the barrier phases are at 5V.

3. Diffusion in the field-free region

At low bias voltages, the substrate is not fully depleted. For most optical wavelengths and in particular for the blue, light is absorbed very close to the back surface, and carriers freely diffuse through the undepleted substrate until they cross the interface, encounter an electric field, and travel to the CCD potential wells. Since the recombination time is very long compared with the diffusion time, recombination may be neglected. We thus consider a point source of charge carriers at the rear surface of a CCD with a field-free thickness y_{ff}. Carriers are reflected from the rear surface, so the problem is equivalent to one with the source at the center of the field-free substrate with thickness $2y_{ff}$. The steady-state solution for the charge distribution $q(\rho, z)$ in the region is obtained by solving Laplace's equation, with the boundary conditions that the source is a δ function at the origin and $q(\rho, \pm y_{ff}) = 0$. The desired current into the depleted region is proportional to $\partial q/\partial z|_{z=y_{ff}}$.

We recognize this as equivalent to the potential problem in which a charge Q is equidistant between two earthed planes at $z = \pm y_{ff}$ [13]. In this case the normal derivative at the plane gives the electric field, which is in turn proportional to the charge density on the plate. This is a well-studied problem. In particular, Jackson [14] gives two solutions, in his problems 3.17(b) and 3.18(b). For unit total charge on each plane (two unit charges at the origin), we obtain

$$\begin{aligned} q(x) &= -\frac{1}{2\pi}\int_0^\infty dk \frac{kJ_0(kx)}{\cosh x} \\ &= -\frac{1}{2}\sum_{m=1}^{\infty}(-1)^m(2m-1)K_0\left((m-\tfrac{1}{2})\pi x\right) \end{aligned} \quad (7)$$

where J is the Bessel function regular at the origin, K is the modified Bessel function which is 0 at infinity, and $x = \rho/y_{ff}$. This corresponds to Hopkinson's $z_s = d$ case[11].

It turns out that the integral form converges rapidly for small x, and only a few terms of the second form are necessary for larger arguments. For example, 7-place accuracy is obtained with 8 terms for $x > 0.5$, while only 2 terms are necessary for $x > 2$. We therefore used both forms to compute $q(x)$, which is shown in Fig. 2. With the function normalized as above, to give a unit charge when integrated over the plane, the amplitude at the origin is a pure number, 0.14568046... [15]. The area of the one-dimensional half-function shown in Fig. 2 is 0.25 [15]. The half-height is at $x = 0.72058$. Since $K_0(x) \to e^{-x}\sqrt{\pi/2x}$ for large x, the standard deviation is finite. Its value is 0.8616. For comparison, the Gaussian with the same half-height (full width at half-maximum) is also shown; it has $\sigma = 0.6120$.

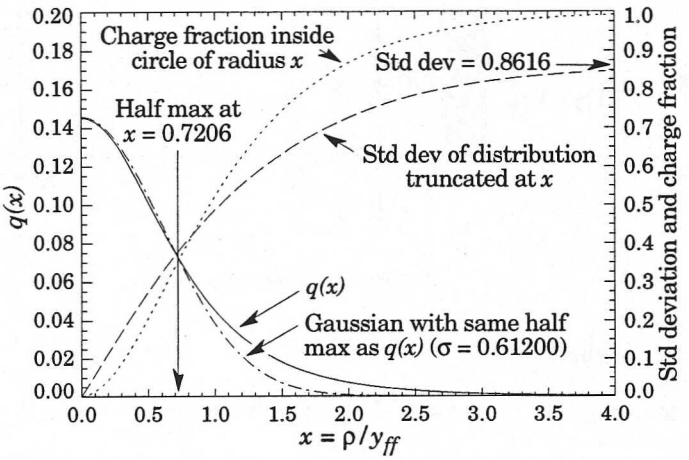

Figure 2: The radial charge distribution $q(x)$ (solid curve) as a function of the scaled variable $x = \rho/y_{ff}$, where y_{ff} is the thickness of the field-free (undepleted) region. It is normalized so that $\int_0^\infty q(x)2\pi x dx = 1$; $\int_0^\infty q(x)dx = 1/4$. For the 1-dimensional distribution ($q(-x) = q(x)$), $\sigma = 0.8616$ and half-maximum is at $x_{1/2} = 0.7206$. Also shown is an (unnormalized) Gaussian distribution (dash-dotted) with the same half-maximum; it has $\sigma = 0.61200$. The standard deviation of the truncated distribution is $\int_{-x}^{x} u^2 q(u)du / \int_{-x}^{x} q(u)du$.

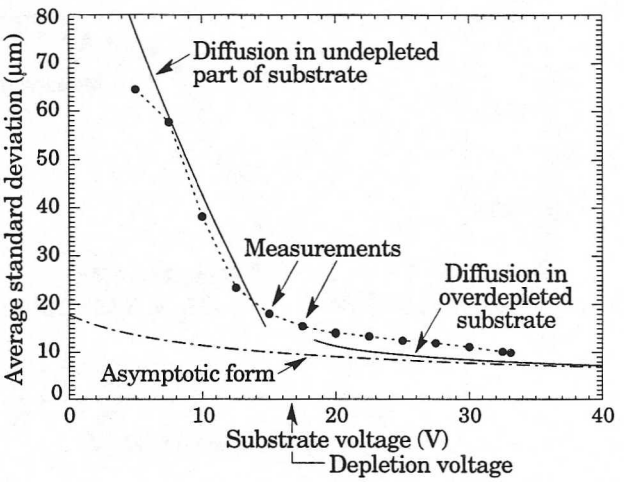

Figure 3: Measured standard deviation for a point light source on back of the CCD. In the present analysis, undersampling results in an overestimate of σ for $\sigma \lesssim 15$ μm. We compare calculated standard deviations for the overdepletion case, and for underdepletion where σ is dominated by diffusion in the undepleted region. The parameters are chosen using the analysis shown in Fig. 4.

The user is cautioned that a fit yielding the full-width at half-maximum will produce a standard deviation which is only 0.7103 as large as the standard deviation calculated from the actual distribution.

4. Experimental results

Charge diffusion has been characterized by imaging a pinhole mask consisting of small openings etched in a chrome layer on a quartz substrate that is placed directly on a back-illuminated CCD [2]. A filter centered at 400 nm was used to give short-wavelength light which is absorbed within 0.1–0.2 μm from the surface. Fig. 3 shows the measured rms charge spreading as a function of substrate bias voltage. In the field region (high $V_{\rm sub}$) this is just the standard deviation of the Gaussian distribution. However, as discussed in the previous section, in the field-free region (low $V_{\rm sub}$) the distribution is not Gaussian and has wide skirts. In addition, undersampling leads to an overestimate of the rms width for $\sigma \lesssim 15$ μm; a reanalysis is in progress.

Also shown in Fig. 3 are the model calculations. The solid line at high $V_{\rm sub}$ is Eq. 3, which requires knowledge of N_D and V_J. These are determined from the data in the low-field region where the charge spreading is given by

$$\sigma_{\rm total}{}^2 = \sigma_{ff}{}^2 + \sigma_f{}^2 \qquad (8)$$

where $\sigma_{ff}{}^2$ and $\sigma_f{}^2$ are the second moments in the field-free and field regions, respectively. At low $V_{\rm sub}$, the $\sigma_{ff}{}^2$ term dominates, which is simply $(0.8616\, y_{ff})^2$. The dependence of y_{ff} on $V_{\rm sub}$ is

$$y_{ff} = y_N - \sqrt{\frac{2\epsilon_{\rm Si}}{qN_D}(V_{\rm sub} - V_J)} \qquad (9)$$

and a plot of $(y_N - y_{ff})^2$ versus $V_{\rm sub}$ should yield a straight line from which N_D and V_J can be determined. The data of Fig. 3 are replotted in Fig. 4. For the data point corresponding to the lowest $V_{\rm sub}$ the second moment was difficult to determine due to overlapping charge distributions from adjacent pinholes. The values determined from Fig. 4 were used to generate the theoretical curves in Fig. 3. Eq. 3 underestimates the measured σ although the trend is basically correct. As mentioned previously, we believe some of the discrepancy results from undersampling due to the pixel size of $(15\ \mu{\rm m})^2$, and this is under investigation. For many astronomical applications a σ value of 10 μm is not a major concern.

5. Conclusions

We have modeled charge spreading in a back-illuminated, fully-depleted CCD. The theoretical charge distribution in the undepleted region is not Gaussian and has long tail regions. The standard deviation for such a distribution has been derived. This information along with experimental data is used to calculate model parameters for the case of overdepletion, where simple transit-time models derived from the theoretical field profile are used to model the diffusion. Comparison with experimental data has been presented with reasonable agreement.

6. Acknowledgments

This work was supported by the U.S. Department of Energy under contract No. DE-AC03-76SF00098. One of the

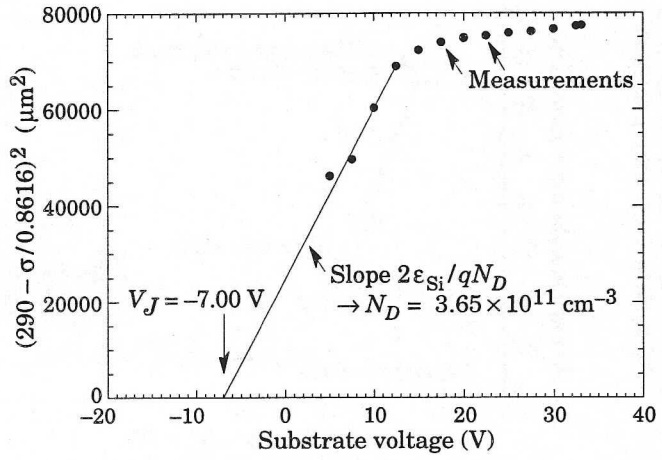

Figure 4: $(y_N - y_{ff})^2$, as estimated from the observed rms deviation as a function of bias voltage. If diffusion in the undepleted region dominates, this quantity should be linear in the bias voltage, with intercept equal to the effective junction potential V_J and slope inversely proportional to N_D, the substrate doping.

authors (DEG) would like to acknowledge useful discussions with J.D. Jackson of the Lawrence Berkeley National Laboratory.

Appendix: Derivation of potentials and fields for an overdepleted CCD

Fig. 5 shows the cross-section of the CCD. The origin is taken at the silicon-SiO_2 interface. The gate insulator thickness is d, the junction depth is at y_J, and the thickness of the substrate is $y_J + y_N$. The solutions to Poisson's equation subject to the boundary conditions $V(-d) = V_G - V_{FB}$, $V(y_J + y_N) = V_{\rm sub}$, and continuity of electric field and potential at y =0 and y_J are [16]

$$V(y) = V_G - V_{FB} - E_{SiO_2}(y+d) \qquad -d < y < 0 \quad (A1)$$

$$V(y) = V_{\rm min} + \frac{qN_A}{2\epsilon_{\rm Si}}(y-y_P)^2 \qquad 0 < y < y_J \quad (A2)$$

$$V(y) = V_J - \frac{qN_D}{2\epsilon_{\rm Si}}(y-y_J)^2 - E_J(y-y_J) \qquad y_J < y < (y_J+y_N) \quad (A3)$$

where $V_J \equiv V(y_J)$, $V_{\rm min} \equiv V(y_P)$, i.e. y_P is the location of the potential minimum, and the electric fields are defined by

$$E_{SiO_2} \equiv -\frac{dV}{dy}(0^-) \quad (A4)$$

$$E_J \equiv -\frac{dV}{dy}(y_J) = -\left(\frac{V_{\rm sub}-V_J}{y_N} + \frac{1}{2}\frac{qN_D}{\epsilon_{\rm Si}}y_N\right) \quad (A5)$$

where the boundary condition $V(y_J+y_N) = V_{sub}$ was used to determine E_J. In terms of terminal voltages E_J is

$$E_J = \frac{V_G - V_{FB} - V_{SiO_2}{}' - V_J{}' - V_{\rm sub}}{y_J + y_N + (\epsilon_{\rm Si}/\epsilon_{SiO_2})\,d} \quad (A6)$$

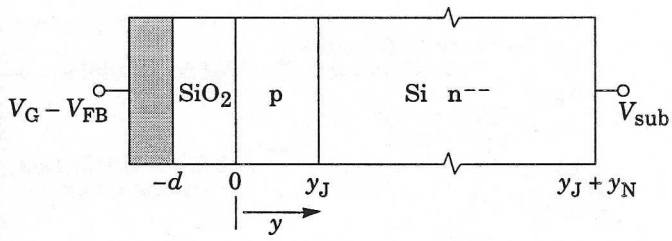

Figure 5: CCD cross section.

where

$$V_{SiO_2}{}' \equiv \frac{qN_A}{2\epsilon_{\rm Si}}y_J{}^2\left(1 + \frac{2\epsilon_{\rm Si}d}{\epsilon_{SiO_2}y_J}\right) \quad (A7)$$

$$V_J{}' \equiv \frac{qN_D}{2\epsilon_{\rm Si}}y_N{}^2 \quad (A8)$$

For the CCDs considered here, $y_N \gg y_J + (\epsilon_{\rm Si}/\epsilon_{SiO_2})\,d$, and Eq. 6 results from Eq. A5 and A6.

References

[1] S.E. Holland *et al.*, *IEDM Technical Digest*, 911, (1996).

[2] R.J. Stover *et al.*, to be published in *Proc. SPIE*, **3019**, (1997).

[3] B.E. Burke, R.W. Mountain, P.J. Daniels, M.J. Cooper, and V.S. Dolat, IEEE Trans. Nucl. Sci., **41**, 375 (1994).

[4] B.E. Burke *et al.*, IEEE Trans. Electron Devices, **38**, 1069 (1991).

[5] S.R. Kamasz, M.G. Farrier, and C.R. Smith, *Proc. SPIE*, **2172**, 76 (1994).

[6] H.Y. Tsoi, J.P. Ellul, M.I. King, J.J. White, and W.C. Bradley, IEEE Trans. Electron Devices, **32**, 1525 (1985).

[7] S.E. Holland, N.W. Wang, and W.W. Moses, to be published in IEEE Trans. Nucl. Sci.

[8] D.M. McCann *et al.*, *Proc. SPIE*, **217**, 118 (1980).

[9] M.C. Peckerar, D.H. McCann and L. Yu, Appl. Phys. Lett., **39**, 55, (1981).

[10] W. Shockley, *Electrons and Holes in Semiconductors*, D. Van Nostrand, New York, 349, (1950).

[11] G.R. Hopkinson, Optical Engineering, **26**, 766, (1987).

[12] J. Janesick *et al.*, *Proc. SPIE*, **597**, 364, (1985).

[13] G.R. Hopkinson, Nucl. Instrum. Meth., **216**, 423, (1983).

[14] J. D. Jackson, *Classical Electrodynamics*, 2nd ed., John Wiley & Sons, New York, (1975).

[15] I. S. Gradshteyn and I. M. Ryzhik, *Table of Integrals, Series, and Products*, trans. Alan Jeffrey, Academic Press (1965); see 3.521.2, 6.511.1, and 3.511.1.

[16] S. M. Sze, *Physics of Semiconductor Devices*, 2nd ed., John Wiley & Sons, New York, 423, (1981).